Accepted for publication in *Nature Ecology and Evolution* published by Springer Nature

Ecology directs host-parasite coevolutionary trajectories across *Daphnia*-microparasite populations

Authors: Sam Paplauskas[1], June Brand[1], Stuart K. J. R. Auld*[1]

[1]Biological & Environmental Sciences, University of Stirling, Stirling, United Kingdom**.** *Correspondence to: s.k.auld@stir.ac.uk.

Host-parasite interactions often fuel coevolutionary change. However, parasitism is one of a myriad of possible ecological interactions in nature. Biotic (*e.g.*, predation) and abiotic (*e.g.*, temperature) variation can amplify or dilute parasitism as a selective force on hosts and parasites, driving population variation in (co)evolutionary trajectories. We dissected the relationships between wider ecology and coevolutionary trajectory using 16 ecologically complex *Daphnia magna-Pasteuria ramosa* ponds seeded with an identical starting host (*Daphnia*) and parasite (*Pasteuria*) population. We show, using a time-shift experiment and outdoor population data, how multivariate biotic and abiotic ecological differences between ponds caused coevolutionary divergence. Wider ecology drove variation in host evolution of resistance, but not parasite infectivity; parasites subsequently coevolved in response to the changing complement of host genotypes, such that parasites adapted to historically resistant host genotypes. Parasitism was a stronger interaction for the parasite than for its host, likely because the host is the principal environment and selective force, whereas for hosts, parasite-mediated selection is one of many sources of selection. Our findings reveal the mechanisms through which wider ecology creates coevolutionary hotspots and coldspots in biologically realistic arenas of host-parasite interaction, and sheds light on how the ecological theatre can affect the (co)evolutionary play.

One sentence summary: Ecological factors affect host-parasite coevolution.

Parasites are a strong selective force acting on host populations, and *vice versa*[1,2], fuelling rapid cycles of adaptation and counter-adaptation in terms of host resistance and parasite capacity to infect[2–5]. These coevolutionary processes can have profound effects on disease outbreaks. For example, whether the host or the parasite is ahead in the coevolutionary process can, in part, affect whether epidemics are emerging[6] or in decline[7]. A key aim of evolutionary ecologists is to understand the extent to which coevolution is: (1) a deterministic process with repeated, predictable outcomes that are either hard-wired or shaped by measurable abiotic and biotic ecological variation; and (2) a stochastic process driven by unpredictable events.

Ecological variation is known to have strong effects on coevolution[8–10]. However, dissecting host-parasite coevolution in biologically realistic settings is fraught with difficulty, and much of our understanding of coevolution therefore comes from laboratory experiments that eliminate ecological complexity. This experimental control comes at a cost to biological realism, because parasitism is just one of many ecological interactions that hosts experience in the wild; predation, competition *etc.*, and abiotic variables such as temperature are already known to either amplify or diminish host evolutionary responses to parasite-mediated selection[4,11–15]. By contrast, we expect parasite evolution, particularly for obligate endoparasites, to be driven primarily by shifts in host-mediated selection caused by changes in host genotype frequencies[16], because hosts insulate their endoparasites from the wider environment. These asymmetries in host and parasite responses to reciprocal selection could create discrepancies between coevolution observed in the laboratory and in the natural arena.

We quantified how coevolutionary trajectories varied among 16 biologically realistic pond populations of *Daphnia magna* and its sterilizing bacterial endoparasite, *Pasteuria ramosa*. Each pond was initiated with an identical suite of *Daphnia* genotypes and the same starting population and dose of *Pasteuria* transmission spores, and the densities of healthy and parasite-infected were then monitored weekly over the course of each pond epidemic. At the end of the epidemic, *Daphnia* were sampled to determine the change in genotype frequencies and additional infected *Daphnia* were sampled to obtain parasite isolates from each pond. We subsequently conducted a time-shift experiment where we exposed replicates of the original twelve *Daphnia* genotypes to either the ancestral parasite used to initiate the pond populations, or to parasite isolates collected from each pond at the end of the epidemic.

By combining data from the time-shift experiment with changes in relative genotype frequencies, we dissected, for each pond, the effects of the three components of host-parasite coevolution on the change in parasite transmission rate over the course of the season: host evolution of resistance, parasite evolution of infectivity, and coevolution (*i.e.*, the extent to which the parasite population non-additively evolved in response to a changed complement of host genotypes). When host genotypes that were resistant to the ancestral parasite increased in frequency within a population, that host population evolved host resistance; when a parasite sample collected at the end of the season caused more infections than the ancestral parasite when exposed to the panel of host genotypes, that parasite population evolved increased infectivity; and when a parasite sample collected at the end of the season became proportionately more infectious to host genotypes that were resistant to the ancestral parasite, that parasite population coevolved in response to the changing complement of host genotypes.

Results and Discussion

Coevolutionary trajectories varied among ponds. Whilst the ponds had the same starting populations of hosts and parasites, each pond experienced its own natural temperature profile (with significant variation across ponds), and half underwent an experimental manipulation of within-population flux (mixing) that simulated extreme precipitation events. We recorded the natural variation in 10 biotic and abiotic ecological variables over the season: temperature, pH, dissolved oxygen, chlorophyll, nitrate, and total dissolved salt, parasite prevalence, predator density and adult host density. This allowed us to examine the role of ecological variation early in the season in driving coevolutionary divergence.

We found that each pond population followed its own coevolutionary trajectory (with respect to changes in parasite transmission rate). This was driven by variation in all three coevolutionary axes: host evolution, parasite evolution and coevolution (Fig. 1a-c). We uncovered asymmetry in the magnitude of host and parasite evolution: parasite populations evolved more in their capacity to infect the ancestral host population than their corresponding hosts evolved capacity to resist the ancestral parasite population (paired t = -3.25, P = 0.005; Fig. 1). We also found a strong positive relationship between the change in host resistance and coevolution, *i.e.*, a change in transmission rates due to a shifting complement of host genotypes (r_s = 0.69, P = 0.004; Fig. 1b): over the course of the season, parasites became disproportionately better at infecting those host genotypes that were previously resistant at the beginning of the season (host genotypes that had become more common), and also disproportionately poorer at infecting host genotypes that were previously susceptible at the beginning of the season (host genotypes that had become rarer). By contrast, there was a lack of relationship between the change in parasite infectivity and coevolution (r_s = 0.39, P =

0.135; Fig. 1c). These findings are consistent with the idea that ecological interactions above and beyond parasitism can select on hosts, but do not act on the host insulated parasites; shifts in host genotype frequencies instead drive parasite genetic change *via* coevolution. Whereas, for ectoparasites, which live on the host exterior, wider ecological conditions are known to shape the evolution of virulence[17,18].

Ecology drives variation in coevolution. Initial inspection of the ten ecological variables in isolation revealed that the mixing treatment had no effect on nine of the ten ecological variables, but that it was associated with lower total adult host densities (see Table S1). This supports the idea that the mixing treatment affected the ecology of the system primarily by reducing host densities directly; indeed, it is known that sediment suspension can interfere with *Daphnia* filter feeding, reducing population growth and the consumption of algae[19] (see later results). Higher temperatures and lower chlorophyll concentration, dissolved oxygen and pH were each associated with the evolution of host resistance, but none of the ecological variables were associated with parasite evolution or coevolution (see Table S2).

However, a more holistic multivariate analysis uncovered a much more interesting story. A Principal Components Analysis of the biotic and abiotic variables (Fig. S1) revealed considerable ecological variation among populations, with the first and second PC axes explaining 36.0% and 21.6% of that variation. The main factors driving variation in unmixed populations were mean temperature and host density, whereas several factors explained variation in mixed populations: chlorophyll, predator density, oxygen, pH and nitrate. There was a strong positive relationship between $\delta_{eco}$the pairwise Mahalanobian distances between populations in multivariate space for ecological variation, and δ_{coevo}, the pairwise Mahalanobian distances for coevolutionary net change (Fig. 2: Mantel r = 0.36, P = 0.029).

126 Populations that were more ecologically different from each other had more divergent
127 coevolutionary trajectories. Both theory[20] and empirical data (reviewed in[10]) have
128 previously shown how host and parasite genotypes can differentially respond to
129 particular environmental variation to create (co)evolutionary hotspots and coldspots[21];
130 these results show how such environmental variables can act in concert to mediate
131 coevolution.

132 **Ecology affects host evolution, with consequences for coevolution.** The next step
133 was to dissect precisely how ecological variation and coevolutionary change were
134 linked. Using Structural Equation Modelling (SEM; Fig. S3), we tested which of two
135 credible scenarios better explained the relationship between ecological and
136 coevolutionary variation among populations (Fig. 3). Scenario 1 (SEM1) proposed
137 that mixing affected ecology (measured as PC1), that ecology directly affected host
138 evolution, parasite evolution and coevolution, and that parasite evolution also
139 separately affected coevolution. Scenario 2 (SEM2) was similar, except it proposed
140 that ecology did not affect coevolution directly; here ecological effects on coevolution
141 were mediated by both host evolution and parasite evolution (see methods section for
142 details). Whilst both SEM1 and SEM2 both provided adequate fit to the data (SEM1:
143 Fisher's C = 19.80, D.F. = 12, P = 0.071, BIC = 64.16; SEM2: Fisher's C = 12.66,
144 D.F. = 12, P = 0.394, BIC = 57.02), SEM2 was the better performing model (ΔBIC =
145 7.14), demonstrating that there was greater support for the scenario where ecological
146 effects on coevolution were mediated by both host evolution and parasite evolution.

147 Analysis of SEM2 revealed that ecological conditions, as expressed by PC1, were
148 significantly different between mixed and unmixed populations (Fig. 3; Fig. 4a; Table
149 S3), and that epidemic size was negatively associated with this measure of ecological
150 variation (Fig. 4b; Table S3), such that epidemics were larger in populations that were

151 warmer, had lower chlorophyll concentrations, lower pH and lower predator densities.
152 Epidemic size was associated with the evolution of host resistance (reduced
153 transmission rate) (Fig. 4c; Table S3), but there was no compelling evidence for an
154 association between epidemic size and parasite infectivity (Fig. 4d; Table S3), or
155 coevolution (Fig. 4e; Table S3). Ecology was also directly associated with evolution
156 of host resistance (Fig. 4f; Table S3), but not parasite infectivity (Fig. 4g; Table S3).
157 Finally, the ability to examine partial residuals after controlling for other variables (a
158 major advantage of the SEM approach) allowed us to uncover that coevolution was
159 positively associated with both the evolution of host resistance (Fig. 4h; Table S3) and
160 the evolution of parasite infectivity (Fig. 4i; Table S3).

161 These separate effects of epidemic size and wider ecology on host (but not parasite)
162 evolution provide two principal insights. They add support our assertion that hosts are
163 subject to a wide range of selective pressures due to both parasite-mediated selection
164 from disease epidemics and from wider ecology, whereas the parasite's insulation
165 within the host environment and the obligate nature of its relationship with the host
166 ensures the host is the principal agent of selection (hence the relationship between
167 host evolution and coevolution). They also raise the intriguing hypothesis that
168 epidemic size and wider ecology (driven in part by mixing treatment) pull two
169 separate levers to drive host evolution of resistance. First, larger epidemics could have
170 exerted greater parasite-mediated selection for host resistance[13]. Second, populations
171 with greater PC1 values, *i.e.*, lower predation and higher temperatures (and thus
172 higher *Daphnia* reproductive rate), had high population densities[22,23], and therefore
173 likely had a greater capacity to respond to any parasite-mediated selection. This may
174 have fuelled coevolution, driving the divergence in coevolutionary trajectories we see
175 in Fig 1.

The next step is to explain the relationships between host evolution, parasite evolution and coevolution. Previous work demonstrated the Matching Allele Model (MAM) best describes the infection genetics of the *Daphnia-Pasteuria* system[4,24,25]: alleles conferring parasite ability to infect one host genotype often preclude it from infecting other different host genotypes[14]. However, MAM in its purest sense requires just one susceptible host genotype for every infectious parasite genotype[26], but in the *Daphnia-Pasteuria* system, parasite genotypes commonly infect >1 host genotypes and also vary in the number of host genotypes each parasite can infect[27]. This deviation from MAM could potentially explain why coevolution was positively associated with the evolution of host resistance and, to a lesser extent, parasite infectivity (Fig. 4h,i; Table S3): parasite populations that were more infectious to the ancestral complement of hosts were also better at infecting the new complement of hosts, and hosts that got better at resisting the ancestral parasite also got better at resisting the evolved parasite. Reciprocal selection could have acted in two ways. First, general selection could have favoured parasite genotypes that infect the broadest range of host genotypes (and *vice versa* for resistance in host genotypes), and second, specific selection could have separately favoured parasite genotypes that could infect host genotypes that had become particularly common (again, *vice versa* for resistance in hosts genotypes).

Conclusion

These results demonstrate that even in seemingly noisy environments, coevolution was still largely driven by deterministic, ecologically-mediated processes. Individual biotic and abiotic variables gave us a small glimpse of how wider ecology shaped coevolution. It was only after viewing multiple ecological variables from a multivariate perspective that we were able to observe that the ecological theatre

determined the (co)evolutionary play in a measurable understandable way (*sensu*[28]). Recent work has demonstrated that quantitative differences among qualitatively similar environments can explain evolutionary divergence among stickleback populations[29]; we show the same is true for more complex host-parasite coevolution, and that knowledge of multiple ecological conditions could help us predict the distribution of coevolutionary hotspots and coldspots[21].

Acknowledgments: We thank Matthew Tinsley, Stephen Thackeray and the Stirling Eco-Evo group for comments on this manuscript. **Funding:** This work was supported by NERC Independent Research Fellowship (NE/L011549/1) and Royal Society Research Grant (RG130657) to S.K.J.R.A. **Author contributions:** Conceptualization: S.K.J.R.A.; data curation: S.K.J.R.A.; formal analysis: S.P., and S.K.J.R.A.; funding acquisition: S.K.J.R.A.; investigation: S.P., J.B., and S.K.J.R.A.; methodology: S.P., J.B., and S.K.J.R.A.; supervision: S.K.J.R.A.; writing original draft: S.P., and S.K.J.R.A; writing, review and editing: all authors. **Competing interests:** All authors declare no competing interests.

References

1. Paterson, S. *et al.* Antagonistic coevolution accelerates molecular evolution. *Nature* **464**, 275–278 (2010).

2. Schulte, R. D., Makus, C., Hasert, B., Michiels, N. K. & Schulenburg, H. Multiple reciprocal adaptations and rapid genetic change upon experimental coevolution of an animal host and its microbial parasite. *Proc. Natl. Acad. Sci. U. S. A.* **107**, 7359–64 (2010).

3. Koskella, B. & Lively, C. M. Evidence for negative frequency-dependent selection during experimental coevolution of a freshwater snail and a sterilizing trematode. *Evolution (N. Y).* **63**, 2213–2221 (2009).

4. Decaestecker, E. *et al.* Host–parasite 'Red Queen' dynamics archived in pond sediment. *Nature* **450**, 870–873 (2007).

5. Gómez, P. & Buckling, A. Bacteria-phage antagonistic coevolution in soil. *Science* **332**, 106–109 (2011).

6. Refardt, D. & Ebert, D. Inference of parasite local adaptation using two different fitness components. *J. Evol. Biol.* **20**, 921–929 (2007).

7. Duffy, M. A., Hall, S. R., Cáceres, C. E. & Ives, A. R. Rapid evolution, seasonality, and the termination of parasite epidemics. *Ecology* **90**, 1441–1448 (2009).

8. Springer, Y. P. Clinical resistance structure and pathogen local adaptation in a serpentine flax-flax rust interaction. *Evolution (N. Y).* **61**, 1812–1822 (2007).

9. Tack, A. J. M., Laine, A.-L., Burdon, J. J., Bissett, A. & Thrall, P. H. Below-ground abiotic and biotic heterogeneity shapes above-ground infection outcomes and spatial divergence in a host-parasite interaction. *New Phytol.* **207**, 1159–1169 (2015).

10. Wolinska, J. & King, K. C. Environment can alter selection in host–parasite interactions. *Trends Parasitol.* **25**, 236–244 (2009).

11. Auld, S. K. J. R., Hall, S. R., Ochs, J. H., Sebastian, M. & Duffy, M. A. Predators and patterns of within-host growth can mediate both among-host competition and evolution of transmission potential of parasites. *Am. Nat.* **184**,

S77–S90 (2014).

12. Wright, R. C. T., Brockhurst, M. A. & Harrison, E. Ecological conditions determine extinction risk in co-evolving bacteria-phage populations. *BMC Evol. Biol. 2016 161* **16**, 227 (2016).

13. Duffy, M. A. *et al.* Ecological context influences epidemic size and parasite-driven evolution. *Science* **335**, 1636–1638 (2012).

14. Auld, S. K. J. R. & Brand, J. Environmental variation causes different (co) evolutionary routes to the same adaptive destination across parasite populations. *Evol. Lett.* **1**, 245–254 (2017).

15. Su, M. & Boots, M. The impact of resource quality on the evolution of virulence in spatially heterogeneous environments. *J. Theor. Biol.* **416**, 1–7 (2017).

16. Auld, S. K. J. R. & Tinsley, M. C. The evolutionary ecology of complex lifecycle parasites: Linking phenomena with mechanisms. *Heredity (Edinb).* **114**, 125–132 (2015).

17. Cardon, M., Loot, G., Grenouillet, G. & Blanchet, S. Host characteristics and environmental factors differentially drive the burden and pathogenicity of an ectoparasite: A multilevel causal analysis. *J. Anim. Ecol.* **80**, 657–667 (2011).

18. Mahmud, M. A., Bradley, J. E. & MacColl, A. D. C. Abiotic environmental variation drives virulence evolution in a fish host–parasite geographic mosaic. *Funct. Ecol.* **31**, 2138–2146 (2017).

19. Arruda, J. A., Marzolf, G. R. & Faulk, R. T. The Role of Suspended Sediments in the Nutrition of Zooplankton in Turbid Reservoirs. *Ecology* **64**, 1225–1235

(1983).

20. Mostowy, R. & Engelstädter, J. The impact of environmental change on host-parasite coevolutionary dynamics. *Proc. R. Soc. B Biol. Sci.* **278**, 2283–2292 (2011).

21. Thompson, J. N. *The Geographic Mosaic of Coevolution* (University of Chicago Press, 2005).

22. Brett, M. T. Chaoborus and fish-mediated influences on Daphnia longispina population structure, dynamics and life history strategies. *Oecologia* **89**, 69–77 (1992).

23. Goss, L. B. & Bunting, D. L. Daphnia development and reproduction: Responses to temperature. *J. Therm. Biol.* **8**, 375–380 (1983).

24. Luijckx, P., Fienberg, H., Duneau, D. & Ebert, D. A matching-allele model explains host resistance to parasites. *Curr. Biol.* **23**, 1085–1088 (2013).

25. Bento, G. *et al.* The genetic basis of resistance and matching-allele interactions of a host-parasite system: The *Daphnia magna-Pasteuria ramosa* model. *PLOS Genet.* **13**, e1006596 (2017).

26. Grosberg, R. K. Mate Selection and the Evolution of Highly Polymorphic Self/Nonself Recognition Genes. *Science* **289**, 2111–2114 (2000).

27. Luijckx, P., Fienberg, H., Duneau, D. & Ebert, D. A Matching-Allele Model Explains Host Resistance to Parasites. *Curr. Biol.* **23**, 1085–1088 (2013).

28. Hutchinson, G. E. *The ecological theater and the evolutionary play* (Yale University Press, 1965).

29. Stuart, Y. E. *et al.* Contrasting effects of environment and genetics generate a continuum of parallel evolution. *Nat. Ecol. Evol.* **1**, 1–7 (2017).

METHODS

Pond experiment. The pond experiment was used to test how epidemic size varied across populations that were initiated with the same suite of hosts and parasites, but experienced biologically realistic variation in biotic and abiotic ecological variables. Additionally, healthy and infected hosts were sampled at the end of the season in order to quantify the change in relative host genotype frequencies across populations and provide parasite samples for the time shift experiment.

To start with, replicate lines of the 12 genotypes of *Daphnia magna* were maintained in the laboratory in a state of clonal reproduction for three generations to reduce variation due to maternal effects. There were five replicates per genotype; each replicate consisted of five *Daphnia* kept in 200 mL of artificial medium[30] modified using 5% of the recommended SeO2 concentration[31]. Replicate jars were fed 5.0 ABS of *Chlorella* vulgaris algal cells per day (where ABS is the optical absorbance of 650 nm white light by the *Chlorella* culture). *Daphnia* medium was changed three times per week and three days prior to the start of the pond experiment. On the day that the pond experiment commenced, 1–3 day old offspring were pooled according to host genotype. Ten offspring per genotype were randomly allocated to each of the 16 ponds (giving a total of 120 *Daphnia* per pond). From preliminary work, we knew that the 12 genotypes used in our pond and laboratory experiments were a representative sample of parasite resistance profiles observed in the source population. The proportion of *Daphnia* that became infected with the ancestral

318 mastermix *Pasteuria* after 48h exposure to 2 x 10^5 spores ranged from 0 to 0.75
319 depending on genotype, with a mean of 0.27.

320 Each pond consisted of a 0.65 m tall 1000 Liter PVC tank filled with rainwater. The
321 ponds were set to different depths into the ground and experienced different
322 temperature profiles[32]. In addition, six of the ponds experienced a weekly mixing
323 treatment where mixed ponds were stirred once across the middle and once around the
324 circumference with a 0.35 m^2 paddle submerged halfway into the pond (the exception
325 to this was on the first day of the experiment, when all ponds experienced the mixing
326 treatment to ensure hosts and parasites were distributed throughout the ponds).

327 The experimental coevolution began on the 2nd April 2015 (Julian day 98), when 120
328 *Daphnia* (10 *Daphnia* x 12 genotypes) and 1 x 10^8 *Pasteuria* spores from the
329 ancestral mastermix were added to each of the 16 ponds. The ancestral mastermix
330 comprised *Pasteuria ramosa* spores propagated using 21 separate *Daphnia* genotypes
331 exposed to sediment from their original pond (Kaimes, Scottish Borders, UK[32]).
332 Between the 2nd April and the 17th November 2015, we measured key abiotic and
333 biotic ecological variables on a weekly basis. Temperature, pH, dissolved oxygen
334 (%), chlorophyll (µg. L^{-1}), nitrate (mg.L^{-1}) and total dissolved salt (mg.L^{-1}) were
335 recorded using an Aquaread AP-5000 probe (Aquaread, Broadstairs, Kent, UK). Host
336 density (L^{-1}), parasite prevalence and predator density (L^{-1}) were determined using
337 standard sampling procedures[32].

338 Twenty-thirty *Daphnia* were sampled from each pond for genotyping after peak
339 epidemic (17th November 2015; Julian Day 321). The DNA extraction and
340 microsatellite genotyping process is described in full in[14]. Microsatellite genotyping

was used to identify the twelve unique multilocus *Daphnia*, and thus track the change in relative genotype frequencies between the beginning of the experiment (when all genotypes were at equal frequencies) and the end of the experiment. The relative genotype frequencies were used as a measure of relative genotype fitness within each pond. Finally, we sampled 90 infected hosts from each of the 16 ponds, which were homogenised and pooled into three replicate isolates per pond (30 infected *Daphnia* per isolate).

Time shift experiment. The time shift experiment was used to understand host and parasite evolution over the course of the epidemic. Specifically, the same panel of host genotypes used to initiate the pond populations was exposed to either the ancestral parasite, or to parasite samples collected from each population at the end of the epidemic, following a fully factorial design.

We established maternal lines for each of the 12 *Daphnia* genotypes used in the pond experiment. There were three replicates per genotype; each replicate consisted of eight adult animals in 100ml of artificial media. The *Daphnia* were fed 0.5 ABS chemostat-grown *Chlorella vulgaris* algae per *Daphnia* per day. Jars were incubated at 20°C on a 12L:12D light cycle, and their media was changed three times per week. Offspring from early instars were taken from the second brood for use in the time shift assay.

The experimental design consisted of a factorial manipulation of the 12 host genotypes and parasite samples collected from each pond (n = 16) plus the original (ancestral) parasite mixed isolate used to seed the populations. There were three independent replicate parasite isolates collected from each pond and a further three replicate isolates of the ancestral parasite (17 parasite treatments; three replicates per

365 treatment). On the day of treatment exposure, neonates from each maternal line were
366 assigned to experimental jars (8 per jar, in 100ml of artificial media) and allocated to
367 parasite treatments following a split-clutch design. There was a total of 612
368 experimental jars (4896 *Daphnia*). Each jar received a dose of 2×10^5 *Pasteuria*
369 spores and kept under identical conditions as the maternal lines. After 48 hours
370 exposure to the *Pasteuria* spores, the experimental *Daphnia* were transferred into
371 fresh media. The infection status of each *Daphnia* was determined by eye 25 days
372 post exposure.

373 Using the results of these infection experiments for each host-parasite combination,
374 we calculated transmission rate (β, L spore^{-1} day^{-1}) using the following equation:

$$\beta = -\frac{1}{Z_0 \cdot t} \cdot \ln\left(\frac{S_t}{S_0}\right) \quad (1)$$

375

376 where Z_0 is the starting density of spores, t is the duration of the trial
377 exposure, S_t is the density of uninfected hosts at the end of the exposure and S_0 is the
378 initial density of hosts.

379 **Dissection of host-parasite (co)evolution.** By combining transmission rate data from
380 the time shift experiment with relative genotype frequency data from the pond
381 experiment, we dissected the various host and parasite contributions towards the
382 evolution of transmission rate.

383 To achieve this, we calculated the change in parasite transmission rate over the course
384 of the season and its three contributory components (eq. 2): change in parasite
385 transmission rate due to evolution of host resistance to the ancestral parasite
386 (hereafter, change in host resistance, $\Delta\beta_h$), change in parasite transmission rate due to

evolution of parasite infectivity to a set of reference hosts (hereafter, change in parasite infectivity, $\Delta\beta_p$), change in parasite transmission rate due to evolution of parasite infectivity to the evolved host population (non-additive coevolution and hereafter, coevolution, $\Delta\beta_{hp}$).

$$\Delta\beta = \Delta\beta_h + \Delta\beta_p + \Delta\beta_{hp} \quad (2)$$

We used two essential pieces of information to determine how host evolution, parasite evolution and coevolution contributed to changes in overall transmission rate for each population: the change in the relative frequency of each host genotype within each population during the course of the pond experiment; and the difference in the susceptibility of these genotypes relative to the ancestral parasite mix used to seed the populations and the parasite samples collected at the end of the epidemic.

First, we calculated the relative frequency of each genotype within each pond at the end of the epidemic. This was done as follows:

$$\overline{w}_{h,t} = P_{h,t} \cdot n_h \quad (3)$$

where $P_{h,t}$ is the frequency of host genotype h at time t, and n_h is the total number of host genotypes used to seed the population (in this case, $n_h = 12$). The coevolution experiment started at $t = 0$, when all hosts had a genotype frequency of 1, and ended at $t = 1$.

Then for each population, we calculated the overall change in mean transmission rate. This was done by determining the change in parasite transmission rate for each host genotype between the end of epidemic parasite samples and the ancestral parasite sample, and weighting by the change in host genotype frequency to calculate a mean for each population:

$$\Delta\beta = \frac{1}{n_h} \cdot \sum_h \left(\left(\beta_{h,t=1} \cdot \bar{w}_{h,t=1} \right) - \beta_{h,t=0} \right), \quad (4)$$

where $\beta_{h,t}$ is the transmission rate of each host genotype.

Next, we calculated the mean change in transmission rate due to population-level evolution of host resistance to the ancestral parasite ($\Delta\beta_h$) by calculating the mean resistance to the ancestral parasite weighted by the change in host relative genotype frequency for each population (eq. 5) and the mean change in transmission rate due to parasite evolution in the capacity to infect the ancestral host population ($\Delta\beta_p$, eq. 6).

$$\Delta\beta_h = \frac{1}{n_h} \cdot \sum_h ((\beta_{h,t=0} \cdot \bar{w}_{h,t=1}) - \beta_{h,t=0}), \quad (5)$$

$$\Delta\beta_p = \frac{1}{n_h} \cdot \sum_h (\beta_{h,t=1} - \beta_{h,t=0}), \quad (6)$$

Finally, we calculated mean change in transmission rate due to host-parasite coevolution (*i.e.*, the non-additive component of disease evolution, $\Delta\beta_{hp}$) using eq. 2.

To visualise how changes in host resistance, parasite infectivity and coevolution covaried, we made bivariate plots of $\Delta\beta_h$, $\Delta\beta_p$ and $\Delta\beta_{hp}$ using vectors.

Quantifying ecological variation among ponds. We calculated mean values (and also variance for temperature) for each of the 10 ecological variables over the early half of the epidemic season (over twelve sampling dates; Julian days 106-200). Initially, we tested the effects of mixing treatment and then fitted separate linear models to examine the relationships between these ten variables and each of $\Delta\beta_h$, $\Delta\beta_p$ and $\Delta\beta_{hp}$; we evaluated the statistical significance of these relationships after applying a sequential Holm-Bonferroni adjustment for multiple comparisons[33]. Next,

we conducted a Principal Components Analysis (using the R function *princomp*[34]) on the ten biotic and abiotic environmental variables to generate a multivariate measure of ecological variation across the pond populations (Fig. S1). We identified the first four principal components as the minimum number of principal components necessary for explaining over 80% of the combined variation, following standard practice[35], and used these in subsequent analyses. For outlier detection, we calculated the squared Mahalanobian distances of each population from the mean and compared these values to the critical threshold for Mahalanobis' distance based on a χ^2 distribution, with a critical α value of 0.05. We found that all populations were below the threshold value for outlier detection and thus all of populations were retained.

Testing for associations between ecological variation and (co)evolutionary trajectories. We conducted two separate analyses to test for relationships between variation in disease coevolutionary trajectories and wider ecological variation. First, we tested whether pairwise differences in ecological conditions among populations were associated with pairwise differences in disease coevolutionary trajectories. We calculated population differences in ecological conditions (δ_{eco}), made up of the first four principal components (over 80% of combined variation), using the Mahalanobian distances between all of the possible pairwise comparisons of populations and the R package StatMatch v1.3.0[36]. We then calculated the overall multivariate distances for net disease coevolution (δ_{coevo}), *i.e.*, differences in change in parasite transmission rates as a composite for differences across three dimensions: host evolution, parasite evolution and coevolution. We then tested for a relationship between δ_{eco} and δ_{coevo} using a Mantel test fitted using the *ecodist* package[37].

Second, we used Structural equation modelling (SEM) to dissect the various relationships between ecological variation, epidemic size and the components of

coevolution. This was done using the *piecewiseSEM* package v2.0.2 in R[38]. SEM allows the evaluation of different causal pathways between variables, and therefore can evaluate support for alternative mediating variables that produce similar associations. We specified two global SEMs (see Fig. S2, Table S3) with the following variables; mixing, ecological variation (PC1 of the previously described PCA), epidemic size, change in host resistance ($\Delta\beta_h$), change in parasite infectivity ($\Delta\beta_p$) and coevolution ($\Delta\beta_{hp}$). The hypothetical causal relationships between the variables included in these SEMs are outlined below:

Mixing: Mixing was an experimental treatment whereby six of the sixteen populations were stirred on a weekly basis. We predicted that this would have a significant effect on the ecological variables. For example, our previous work has shown that mixing significantly changes *Daphnia* host population densities and affects epidemic size[32].

Ecology: Ecological variation was represented by the first principal component (PC1), which explained 36.0 % of the overall variation, extracted from the PCA of the multiple environmental variables measured during the pond experiment. PC1 was mainly associated with low mean temperature, high chlorophyll concentrations and high predator density. The positive effects of temperature and negative effects of predation on parasite prevalence have been well documented in *Daphnia* disease systems[13,32,39,40]. Therefore, we predicted that our measure of ecological variation would be negatively associated with epidemic size and would be associated with the components of transmission rate evolution (changes in host resistance, parasite infectivity and coevolution).

Epidemic size: Epidemic size (integrated parasite prevalence, calculated by integrating the area under the time series of empirically determined prevalence for

each mesocosm) could potentially be both a cause and a consequence of host evolution, parasite evolution and coevolution. There is ample evidence from previous studies that epidemics exert parasite-mediated selection and can cause the evolution of host resistance[41–44], and that rapid host evolution of resistance can bring epidemics to an end[45]. Given the bi-directional relationship between these variables we expected that there would be covariation between epidemic size and changes in host resistance, parasite infectivity and coevolution, but made no prediction about the direction of causality.

Change in host resistance ($\Delta\beta_h$), parasite infectivity ($\Delta\beta_p$), and coevolution ($\Delta\beta_{hp}$): We developed two SEMs to test between two hypothetical relationships between epidemic size, ecology and different aspects of disease evolution. Hypothesis one is that ecology directly drives both epidemic size and all three components of disease evolution (Fig. S2). Hypothesis two is that ecology affects epidemic size, host evolution of resistance and parasite evolution of infectivity, but that decreases in host resistance (*i.e.,* increased transmission rate) should negatively affect coevolution and increases in parasite infectivity should positively affect coevolution. Following our prediction that the wider environment has a greater impact on hosts compared to parasites, we expected that there would be asymmetry in the strength of the relationship between these different components of evolution with coevolution, such that hosts significantly affect coevolution more than parasites.

After fitting the two SEMs, we tested which provided the superior fit using Bayesian Information Criterion (BIC). We chose BIC over Akaike's Information Criterion (AIC) and AIC corrected for small sample sizes (AICc) because BIC has been shown to better predict model performance when there is unobserved heterogeneity in the data[46], which seems highly likely in both our genotype frequency and ecological

variable data. We then conducted Fisher's C tests (Shipley's tests of directed separation[47] on the best-fitting model to discover potentially relevant relationships that had been excluded from the model. Finally, in order to achieve greater statistical power to test the significance of each of the proposed relationships, we divided the best performing global SEM into two submodels. It should be noted that the parameter estimates for each of the unidirectional relationships in the submodels was identical to the corresponding parameter estimates in the global model.

Data availability: All data is available on dryad doi:10.5061/dryad.qv9s4mwd6.

Code availability: All companion code is available on Dryad: doi:10.5061/dryad.qv9s4mwd6. As we are actively researching these datasets, we kindly ask that researchers contact us if they are planning to use the data for reasons other than reproducing the findings of our paper.

The following references appear in the Methods only.

30. Klüttgen, B., Dülmer, U., Engels, M. & Ratte, H. . ADaM, an artificial freshwater for the culture of zooplankton. *Water Res.* **28**, 743–746 (1994).

31. Ebert, D., Zschokke-Rohringer, C. D. & Carius, H. J. Within–and between–population variation for resistance of *Daphnia magna* to the bacterial endoparasite *Pasteuria ramosa*. *Proc. R. Soc. London. Ser. B Biol. Sci.* **265**, 2127–2134 (1998).

32. Auld, S. K. J. R. & Brand, J. Simulated climate change, epidemic size, and host evolution across host–parasite populations. *Glob. Chang. Biol.* **23**, 5045–5053 (2017).

525 33. Holm, S. A simple sequentially rejective multiple test procedure. *Scand. J. Stat.*
526 (1979).

527 34. R Core Team. R: A language and environment for statistical computing.
528 (2019).

529 35. Brereton, R. G. & Lloyd, G. R. Re-evaluating the role of the Mahalanobis
530 distance measure. *J. Chemom.* **30**, 134–143 (2016).

531 36. D'Orazio, M. StatMatch: Statistical Matching or Data Fusion. (2019).

532 37. Goslee, S. C. & Urban, D. L. The ecodist Package for Dissimilarity-based
533 Analysis of Ecological Data. *J. Stat. Softw.* **22**, (2007).

534 38. Lefcheck, J. S. piecewiseSEM: Piecewise structural equation modelling in r for
535 ecology, evolution, and systematics. *Methods Ecol. Evol.* **7**, 573–579 (2016).

536 39. Auld, S. K. J. R., Wilson, P. J. & Little, T. J. Rapid change in parasite infection
537 traits over the course of an epidemic in a wild host-parasite population. *Oikos*
538 **123**, 232–238 (2014).

539 40. Shocket, M. S. *et al.* Parasite rearing and infection temperatures jointly
540 influence disease transmission and shape seasonality of epidemics. *Ecology* **99**,
541 1975–1987 (2018).

542 41. Duncan, A. B., Mitchell, S. E. & Little, T. J. Parasite-mediated selection and
543 the role of sex and diapause in *Daphnia*. *J. Evol. Biol.* **19**, 1183–1189 (2006).

544 42. Auld, S. K. J. R. *et al.* Variation in costs of parasite resistance among natural
545 host populations. *J. Evol. Biol.* **26**, 2479–2486 (2013).

546 43. Laine, A.-L. Evolution of host resistance: looking for coevolutionary hotspots

at small spatial scales. *Proceedings. Biol. Sci.* **273**, 267–73 (2006).

44. Lohse, K., Gutierrez, A. & Kaltz, O. Experimental evolution of resistance in *Paramecium Caudatum* against the bacterial parasite Holospora Undulata. *Evolution (N. Y).* **60**, 1177 (2006).

45. Duffy, M. A. & Sivars-Becker, L. Rapid evolution and ecological host-parasite dynamics. *Ecol. Lett.* **10**, 44–53 (2007).

46. Brewer, M. J., Butler, A. & Cooksley, S. L. The relative performance of AIC, AIC C and BIC in the presence of unobserved heterogeneity. *Methods Ecol. Evol.* **7**, 679–692 (2016).

47. Shipley, B. A New Inferential Test for Path Models Based on Directed Acyclic Graphs. *Struct. Equ. Model. A Multidiscip. J.* **7**, 206–218 (2000).

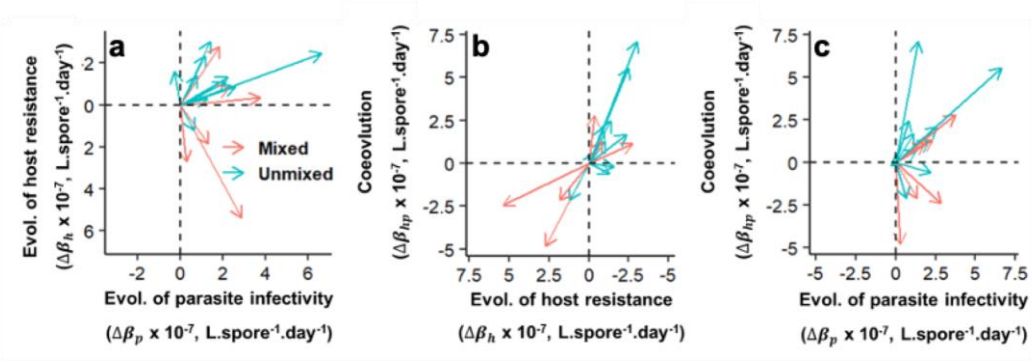

560

561 **Fig. 1. Coevolutionary trajectories vary across populations.** Vectors show pairwise
562 relationships between **a** change in transmission rate due to host evolution of resistance
563 ($\Delta\beta_h$) and change in transmission rate due to parasite evolution of infectivity ($\Delta\beta_p$), **b**
564 host evolution of resistance ($\Delta\beta_h$) and non-additive change in transmission rate due to
565 coevolution ($\Delta\beta_{hp}$) and **c** parasite evolution of infectivity ($\Delta\beta_p$) and coevolution
566 ($\Delta\beta_{hp}$). Populations were identical pre-epidemic (vector tails) and by the end of the
567 epidemic phenotypes had diverged due to variation in evolutionary trajectories (vector
568 heads, open arrowheads). Red arrows denote populations that underwent the mixing
569 treatment and blue arrows denote populations that remained unmixed.

570

571

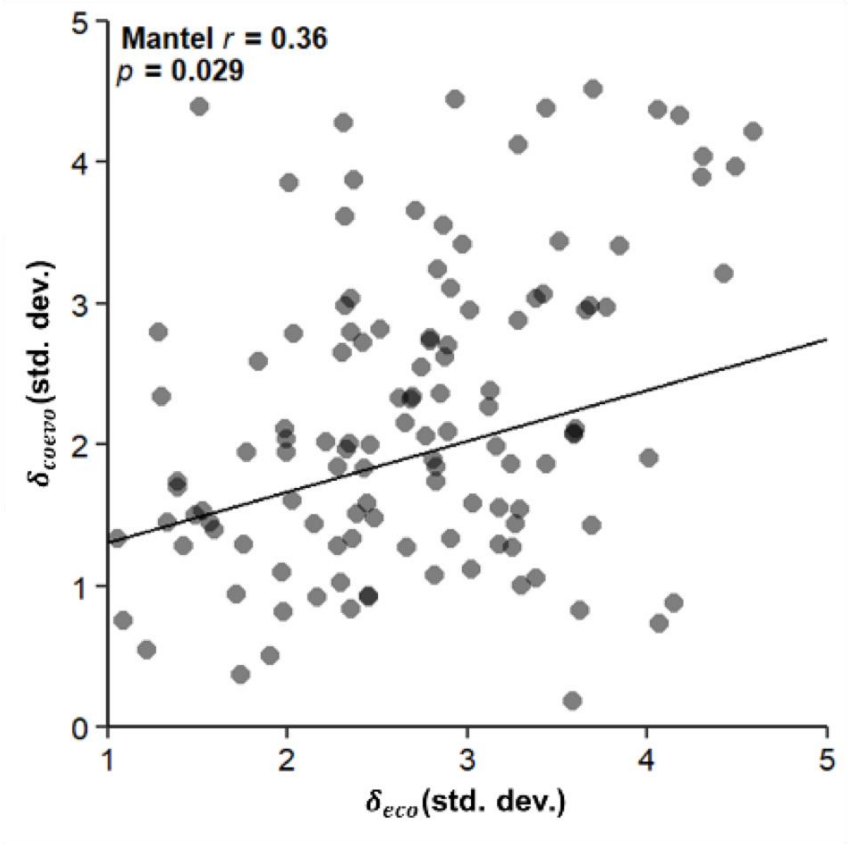

572
573 **Fig. 2. Pairwise ecological differences explain population divergence in**
574 **coevolutionary trajectory.** Relationship between pairwise population distances
575 (measured as Mahalanobis distances) for ecology (across PC1-PC4, δ_{eco}) and net
576 coevolutionary trajectory (combining the three axes of host evolution, parasite
577 evolution, coevolution, δ_{coevo}). Pairwise differences are measured in standard
578 deviations of the total variation.

579

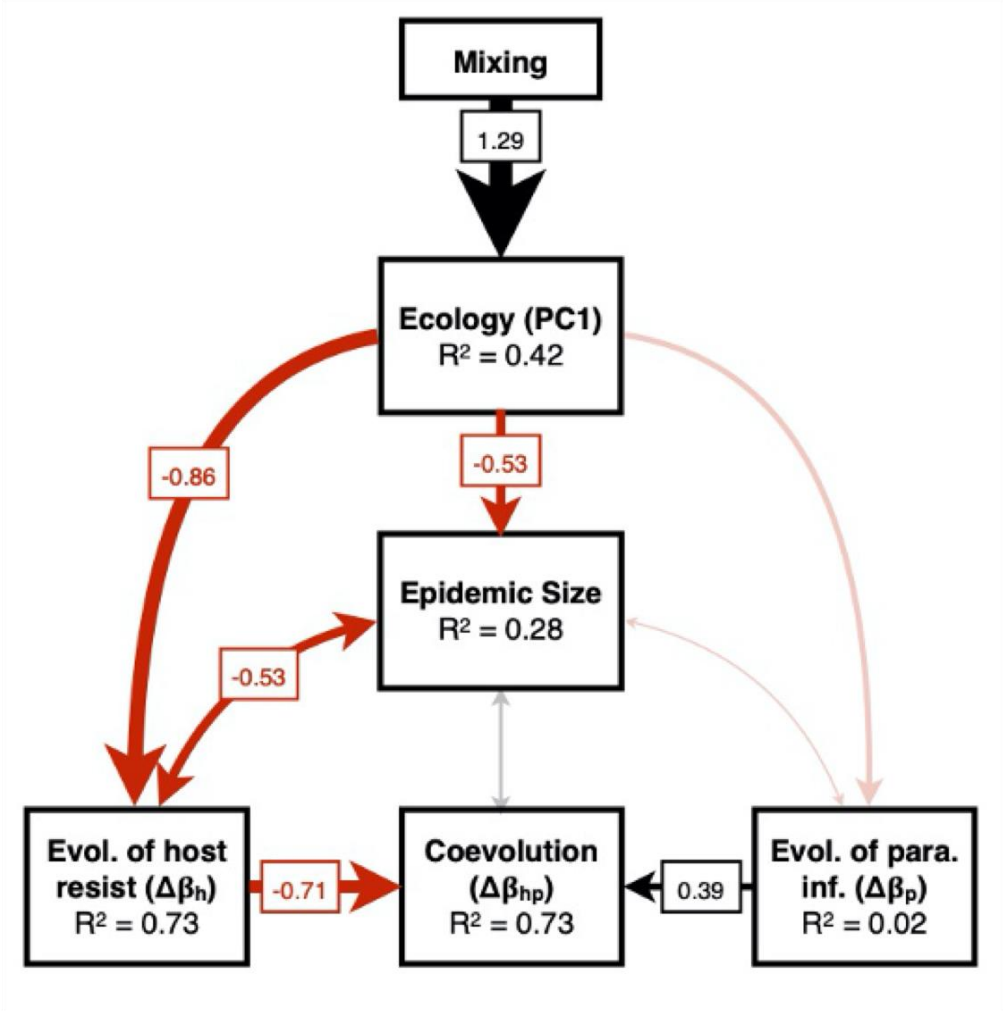

580

581 **Fig. 3. Wider ecology drives coevolution through its effects on host evolution.**

582 Path diagram for SEM2 showing how ecology drives coevolution. Arrows represent

583 unidirectional (single arrowhead) or bidirectional (double arrowheads) relationships.

584 Black arrows denote positive relationships, red arrows negative ones. Significant

585 (p<0.05) and non-significant relationships are represented by solid and partially

586 transparent arrows respectively. The arrow width of significant relationships is scaled

587 according to the standardised regression coefficient shown in the small boxes (see

588 also Fig. 4, Table S3). Note that negative values of $\Delta\beta_h$ represent evolution of host

589 resistance.

590

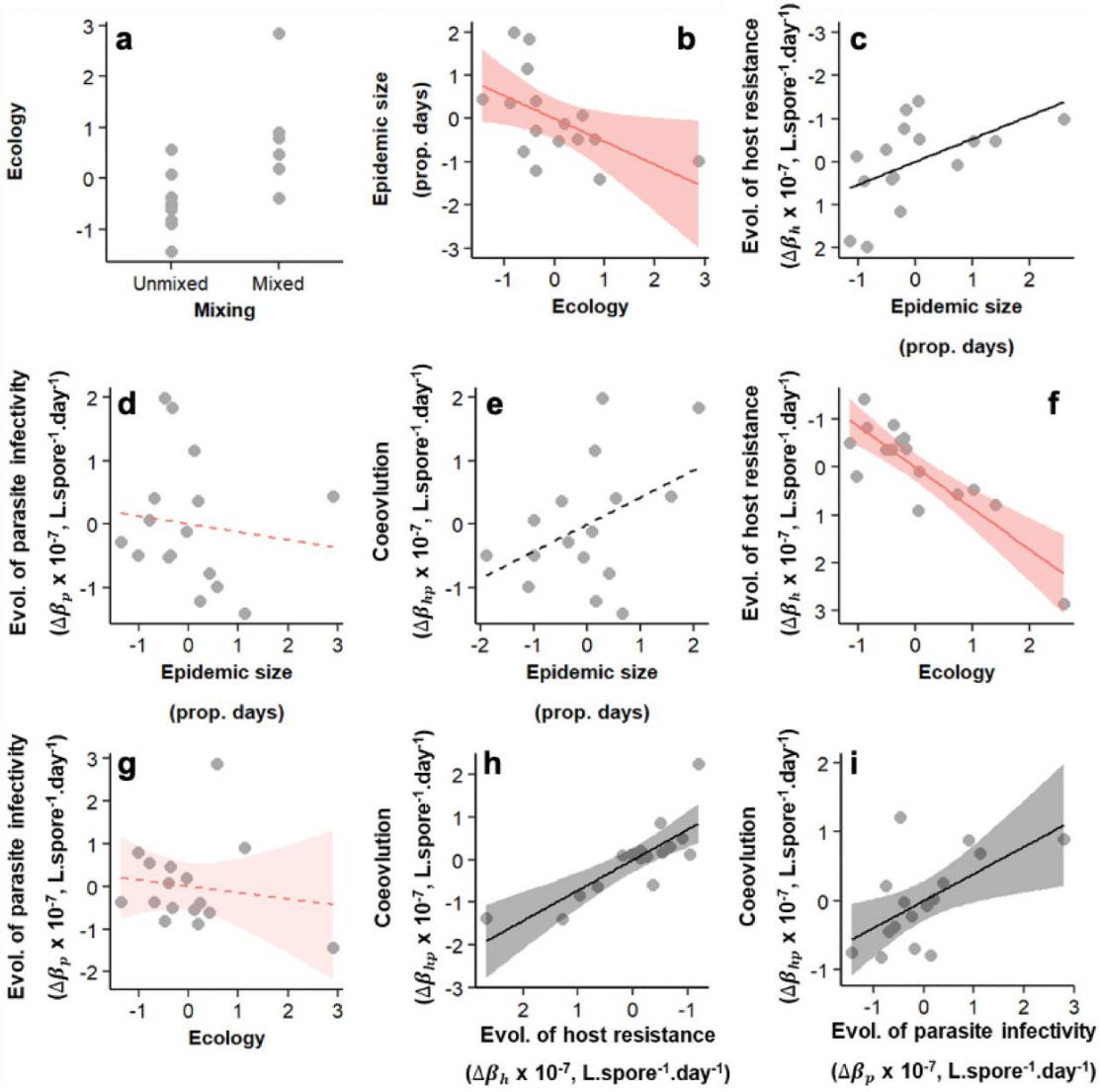

Fig. 4. Ecological, epidemiological and coevolutionary relationships across populations. Relationships between variables from SEM2 **a-i**. Colours show positive (black) and negative (red) relationships, and bands denote 95% CIs. Note that negative values of $\Delta\beta_h$ represent evolution of host resistance. Significant (p>0.05) and non-significant relationships are indicated by solid and dashed lines respectively.